Overexpression of Astroglial Major Histocompatibility Complex Class I in the Medial Prefrontal Cortex Impairs Visual Discrimination Learning in Mice

Bolati Wulaer
Nagoya University Graduate School of Medicine
Kazuhiro Hada
Nagoya University Graduate School of Medicine
Akira Sobue
Nagoya University Graduate School of Medicine
Norimichi Itoh
Nagoya University Graduate School of Medicine
Toshitaka Nabeshima
Fujita Health University Graduate School of Health Science
Taku Nagai
Nagoya University Graduate School of Medicine
kiyofumi yamada (kyamada@med.nagoya-u.ac.jp)
Nagoya University

Research

Keywords: MHCI, astrocyte, touchscreen, visual discrimination, reversal learning, learning and memory, cognition, sociality, recognition memory, clozapine

Posted Date: May 12th, 2020

DOI: https://doi.org/10.21203/rs.3.rs-27601/v1

Version of Record: A version of this preprint was published at Molecular Brain on December 1st, 2020.
See the published version at https://doi.org/10.1186/s13041-020-00710-5.

Abstract

Background Immune molecules, such as cytokines, complement, and major histocompatibility complex (MHC) proteins, in the central nervous system are often associated with neuropsychiatric disorders. Neuronal MHC class I (MHCI), such as H-2D, regulate neurite outgrowth, the establishment and function of cortical connections, and activity-dependent refinement in mice. We previously established mice expressing MHCI specifically in astrocytes of the media prefrontal cortex (mPFC) using the adeno-associated virus (AAV) vector under the control of the glial fibrillary acidic protein (GFAP) promoter. Mice expressing the soluble form of H-2D (sH-2D) in the mPFC (sH-2D-expressing mice) showed abnormal behaviors, including social interaction deficits and cognitive dysfunctions. However, the pathophysiological significance of astroglial MHCI on higher brain functions remains unclear. Therefore, cognitive function in mice expressing sH-2D in astrocytes of the mPFC was tested using the visual discrimination (VD) task to assess the impact of the astrocyte pathology and resulting behavioral changes.

Methods Three separate batches of mice were used in the present study. sH-2D-expressing mice were subjected to the VD and reversal learning tasks, morphological analyses, and pharmacological intervention using clozapine in the social interaction and novel object recognition tasks.

Results In pretraining, the performance of sH-2D-expressing mice was normal in response phase sessions (stages 1–4), but impaired in the punish phase session (stage 5). The total numbers of sessions, trials, normal trials, and correction trials to reach the VD criterion were significantly higher in sH-2D-expressing mice than in control mice. A morphological study showed that dendritic complexity was significantly reduced in the dorsal striatum of sH-2D-expressing mice. A treatment with clozapine ameliorated decreased social behavior as well as impaired object recognition memory in sH-2D-expressing mice.

Conclusion Collectively, the present results suggest that the overexpression of astroglial MHCI in the mPFC results in impaired VD learning, which may be accompanied by decreased dendritic complexity in the dorsal striatum and mPFC.

Background

The brain is considered to be ‘immuno-privileged’ because of the lack of classical immune molecules in the central nervous system (CNS) [1, 2]. However, this paradigm shifted to neural immune-based mechanisms for brain functions after the discovery of immune molecules, such as cytokines, complement, and major histocompatibility complex (MHC) proteins, in the developing and adult brain [3–5]. Among these immune molecules, recent studies highlighted the roles of MHC class I (MHCI) in the brain. MHCI molecules contain a heavy chain and β2-microglobulin light chain [6, 7]. In the immune system, MHCI presents a short polypeptide of 8–10 amino acids from a cytosolic antigen when a cell is infected with a virus. These peptides are recognized by the T-cell receptors of cytotoxic T cells, leading to the initiation of an immune response [8, 9]. In the CNS, neuronal MHCI molecules regulate neurite

outgrowth, cortical connections, activity-dependent refinement in the visual system, and plasticity [3–5, 10–12]. Glial MHCI molecules are weakly expressed in normal and healthy brains, but are up-regulated under pathological conditions. A systemic immune stimulation in rodents has been shown to activate astrocytes and microglia in the brain [13, 14] and induce MHCI gene expression in non-neuronal cells [15] and MHCII in microglia [16].

To clarify the pathophysiological role of MHCI expression in astrocytes, we previously established mice expressing MHCI specifically in astrocytes of the medial prefrontal cortex (mPFC) using the AAV vector under the control of the glial fibrillary acidic protein (GFAP) promoter [17]. Mice expressing the soluble form of H-2D (sH-2D) in the mPFC (sH-2D-expressing mice) showed brain dysfunction manifested by impaired social interactions and object recognition memory, which were accompanied by neuropathological changes, including the activation of microglial cells, decreases in parvalbumin-positive cell numbers, and reductions in dendritic spine density in the mPFC. A treatment with GW4869, an inhibitor of exosome synthesis, ameliorated these behavioral and neuropathological changes in sH-2D-expressing mice, suggesting that the overexpression of MHCI in astrocytes affects microglial proliferation as well as neuronal numbers and spine densities, thereby leading to social and cognitive deficits in mice, possibly via exosomes produced by astrocytes [17].

In the present study, we investigated higher brain functions in sH-2D-expressing mice using the VD task to assess the impact of the astrocyte pathology and resulting behavioral changes. The touchscreen-based VD task provides high translational validity to further evaluate neuronal projections for higher-order brain functions in mice [18–22]. Previous studies indicated that the dorsal striatum is important for VD learning [20, 23]. Instrumental action and outcome behaviors are known to depend on the dorsal striatum and its connections with the mPFC [24, 25]. Therefore, we examined the dendritic morphology of medium spiny neurons in mPFC projection terminals, the dorsomedial striatum (DMS), and dorsolateral striatum (DLS) [26]. We also investigated the effects of a pharmacological intervention using clozapine, an atypical antipsychotic drug, to elucidate the relationship between behavioral changes in sH-2D-expressing mice and the clinical symptoms of mental diseases.

Methods

Animals

C57BL/6J mice (Japan SLC, Shizuoka, Japan) were housed and maintained under a standard specific pathogen-free environment with a standard 12-hr light/dark cycle (lights on at 9:00) at a constant temperature of 23 ± 1ºC. Animals were given a 1-week acclimatization period prior to the start of the experiments. They were allowed free access to food and water before the initiation of pretraining for the VD and reversal learning tasks. Only male mice were used in the present study to avoid potential estrus cycle-related performance variability in females [27]. Three separate batches of mice were used in the present study (total of 53 mice). They were randomly subjected to control or sH-2D viral injection groups as follows: VD and reversal learning (Control 4 mice, sH-2D-expressing 4 mice); Golgi staining (Control 4

mice, sH-2D-expressing 4 mice); Clozapine treatment in social interaction and novel recognition tests (control + vehicle n = 10 mice, control + clozapine n = 9 mice, sH-2D + vehicle n = 9 mice and sH-2D + clozapine n = 9 mice). The present study was not pre-registered and no randomization/blinding was performed. No exclusion criteria were predetermined and no animals were excluded. Animals were handled in accordance with the guidelines established by the Institutional Animal Care and Use Committee of Nagoya University, the Guiding Principles for the Care and Use of Laboratory Animals approved by the Japanese Pharmacological Society, and the National Institutes of Health Guide for the Care and Use of Laboratory Animals.

Plasmid and AAV production

We produced the plasmid and AAV as described previously [17]. Briefly, cDNA for mouse MHCI was amplified by polymerase chain reaction (PCR) from a mouse brain cDNA library using specific primers (sH-2D forward primer, ATGAATTCGCCGCCATGGGGGCGATGGC; sH-2D reverse primer, ATGTCGACCCATCTCAGGGTGAGGGGCT), and inserted into a pCRII-blunt TOPO vector (Invitrogen, Carlsbad, CA, USA). cDNA was subcloned into the EcoRI site of the expression vector pCAGGS-HA, which was a gift from Dr. Kozo Kaibuchi. In the AAV vector, pZac2.1 gfaABC1D-EGFP-P2A-sH-2D was generated by replacing EGFP-P2A-sH-2D in tdTomato in pZac2.1-gfaABC1D-tdTomato, which was donated by Dr. Baljit Khakh (Addgene plasmid # 44332). AAV vectors were prepared as described previously [17, 28]. Briefly, plasmids for the AAV vector, pHelper (Cell BioLabs Inc., San Diego, CA), and pAAV-2/5 (Cell BioLabs Inc.) were transfected into HEK293 cells (Cell BioLabs, Inc.) using Lipofectamine 2000 (Invitrogen). After a 3-day incubation, cells were collected and lysed by freeze and thaw cycles. Cell lysates were incubated with benzonase nuclease (Millipore, Darmstadt, Germany). Cell debris was removed by centrifugation at 10,000 x g at room temperature for 10 min. Supernatants were used as the primary virus. AAV titers were estimated via a quantitative polymerase chain reaction.

sH-2D-expressing mouse model

We established the sH-2D-expressing mouse model as described previously (Sobue et al., 2018). Briefly, seven-week-old male mice were anesthetized with tribromoethanol (250 mg/kg, i.p.) and positioned in a stereotaxic frame (David Kopf, Tujunga, CA, USA). AAV gfaABC1D-EGFP-P2A-sH-2D (1×10^{12} genome copies/ml) was bilaterally injected into the mPFC (+ 1.5 mm anteroposterior, ± 0.5 mm mediolateral from the bregma, -2.5 mm dorsoventral from the skull) in a volume of 0.5 µL/site, according to the mouse brain atlas [29]. AAV gfaABC1D-EGFP-P2A was injected as a control group. Three weeks after injections, animals were subjected to behavioral analyses.

Touchscreen-based VD and reversal learning tasks

Tasks were performed using the touchscreen chamber system (Phenosys, Berlin, Germany; Brainscience Idea, Osaka, Japan). The protocol used was described in detail in previous studies [20, 30]. Briefly, access to food and water was restricted for 2 hr each day at least 1 week before pretraining in order to provide sufficient motivation to perform the tasks, and food and water restrictions were continued until the end of the task. The task started with 5-stage pretraining to shape screen-touch behavior in mice (Fig. 1). In

stage 1, mice were habituated to the touchscreen chamber. They were allowed to freely explore the chamber and rewards were available during the 20-min session. The criterion was to receive 30 rewards (20 μl of milk) on 2 consecutive days. During stage 2, one window of the touchscreen was illuminated with a white plain square for 30 seconds (Fig. 1b). When the stimulus was offset, the reward nozzle came into the chamber and the reward was delivered. The retrieval of milk initiated an inter-trial interval (ITI) of 20 seconds before the next image presentation. When the mouse touched the response window during a white plain square presentation, a reward was delivered to accompany the image stimulus termination. Stage 3 proceeded in the same manner as stage 2, except that the mouse was required to touch the response window displaying the image before reward delivery. Each image was displayed until mice touched the response window. The criterion was to receive 30 rewards in a 60-minute session at least once. In addition to the stage 3 procedure, mice had to initiate each trial by approaching the nozzle in stage 4 (Fig. 1c). When the trial started, the nozzle was presented in the operant chamber without a reward. Touching the nozzle resulted in the presentation of an image on the touchscreen. The criterion was the same as that for stage 3. In stage 5, mice were introduced to incorrect responses. Mice were punished for touching a blank response window with a 5-second time-out. ITI began after the time-out, and then the next trial was initiated. The criterion in this stage was to complete 30 rewards showing ≥ 75% accuracy in a 30-minute session on 2 consecutive days, and mice were then moved to the VD task. To prevent location bias, the stimulus was pseudorandomly presented during all training stages; it never showed more than 3 times on the same side in a row. After mice learned how to operate the touchscreen (> 75% on 2 consecutive days), they were subjected to the VD task. In the VD task, trial initiation was triggered by mice touching the nozzle, and 2 stimuli (marble and fan) were then presented simultaneously in the 2 response windows (Fig. 1d). One of the stimuli was associated with a reward, while the other was not. Stimuli were presented pseudorandomly and not displayed in the same location for more than 3 trials in a row (excluding correction trials). Stimulus contingencies were counterbalanced. Touching the correct response resulted in the delivery of a reward (20 μL of milk). When the incorrect response was touched, the stimuli offset immediately and a 5-second time-out period was started. After ITI (20 seconds), a correction trial was given instead of a new trial. In the correction trial, the same stimulus set was repeatedly presented in the same location until the mouse made a correct response. The criterion of the task was a more than 80% correct response on 2 consecutive days. The session finished after 60 minutes or the completion of 30 trials. The total numbers of trials, correction trials, and correction errors as well as the percentage of correct responses and the perseveration index (the number of correction trials as a ratio of errors) in different training stages were analyzed. The reversal learning task was similar to the initial acquisition of the VD task, except that the contingency of the stimulus pair was reversed. Once a mouse reached the criterion, the contingency of the stimuli was reversed. The previous reward stimulus became an incorrect response, while the previous non-rewarded stimulus became the correct response.

Social interaction test

The social interaction test was conducted as described previously [31]. Control and sH-2D-expressing mice were individually housed in a home cage (29 × 18 × 12 cm) for 2 days before the trial. We used age-matched male C57BL/6J mice as intruders that had not shown aggressive behavior. In the first trial (5 min), an intruder mouse was introduced into the resident's home cage. The duration of social interactions (close following, inspection, anogenital sniffing, and other social body contact apart from aggressive behavior) was analyzed. Four trials, with ITI of 30 min, were used to analyze social behavior using the same intruder mouse.

Novel object recognition test

The novel object recognition test was performed as described previously [32]. Mice were individually habituated to an open box (30 × 30 × 35 cm) for 3 days. During the training session, two novel objects were placed in the open-field and mice were allowed to explore for 10 min under moderately lit conditions (15 lx). The time spent exploring each object was recorded. During test sessions, one of the familiar objects used during the training session was replaced by a novel object. Animals were placed back into the same box 24 hr after the training session and allowed to explore freely for 5 min. The preference index in the test session, the ratio of the amount of time spent exploring the novel object over the total time spent exploring both objects, was used to measure cognitive function. In the training session, the preference index was calculated as the ratio of time spent exploring the object that was replaced by a novel object in the test session, to the total exploration time.

Golgi staining and morphological analyses

Golgi staining was performed using the FD Rapid Golgi Stain Kit according to the manufacturer's protocol (FD NeuroTechnologies, Ellicott City, MD, USA) and a previous study [17]. Brains were then sectioned using a cryostat at a thickness of 80 μm. Bright-field microscopic images of neurons located in DMS and DLS were obtained (BZ9000, KEYENCE, Osaka, Japan). Only fully impregnated neurons isolated from neighboring displaying dendritic trees without obvious truncations and impregnated neurons were retained for analyses. All dendrites within images were traced using Neurolucida software (MicroBrightField Bioscience, Williston, VT, USA) and analyzed by NeuroExplorer (MicroBrightField). These analyses were performed using 12 slices per mouse from 4 mice in each group.

Data analyses

All data were expressed as means ± SEM. In pretraining and VD experiments (Fig. 2a-f and 3a-d), differences between two groups were analyzed by a two-tailed Student's t-test. In reversal learning (Fig. 3e and f), the Sholl analysis (Fig. 4), and clozapine treatment in social interaction and novel object recognition tests (Fig. 5), multiple group comparisons were conducted using a one-, two-, or three-way analysis of variance (ANOVA), followed by Tukey's test when F ratios were significant ($*p < 0.05$). An assessment of the normality of data prior to statistical comparisons was not performed; however, this type of analysis is resistant to deviations from the assumptions of the traditional ordinary-least-squares ANOVA and is robust to outliers, and, thus, is insensitive to distributional assumptions (such as

normality) [33]. Data were not assessed for normality or no test for outliers was conducted. The criterion for a significant difference was $p < 0.01$ or $p < 0.05$ for all statistical evaluations.

Results

Performance of sH-2D-expressing mice in pretraining

Mice were initially subjected to pretraining to gradually shape screen-touching behavior [20, 30]. Pretraining consisted of 5 stages (Fig. 1a). White plain and blank stimuli were used in the pretraining stages (Fig. 1b). In stage 1, mice were habituated to the chambers and received liquid rewards in 2 daily sessions. In stage 2, the delivery of the liquid reward was dependent on the approach of a visual stimulus (white plain square) or occurred after the 30-sec presentation. Stage 3 was similar to stage 2; however, the stimulus offset required mice to touch it. Stage 4 was similar to stage 3; however, mice had to trigger stimulus presentation by approaching the reward delivery nozzle (Fig. 1c). As shown in Fig. 2, control and sH-2D-expressing mice required the same number of trials to reach the criterion (receive 30 rewards in a session) in stages 1–4 (Response phase; Fig. 2a-d). In stage 5, mice were discouraged from touching the blank response window during stimulus presentation, with no reward being delivered and a 5-sec time-out period (Punish phase). In this stage, sH-2D-expressing mice required significantly more trials to reach the criterion (to reach 75% accuracy for at least 2 sessions) than control mice ($t(6) = 2.74$, $P = 0.0338$; Fig. 2e). The total number of trials in pretraining sessions was significantly higher for sH-2D-expressing mice than for control mice ($t(6) = 2.74$, $P = 0.0338$; Fig. 2f).

Performance of sH-2D-expressing mice in VD and reversal learning tasks

The VD task was initiated when mice reached the criterion in pretraining. In this task, mice were required to touch a stimulus to obtain the liquid reward from a pair of stimuli (marble and fan; Fig. 1a and d). sH-2D-expressing mice needed significantly more sessions to reach the criterion (reach more than 80% accuracy on 2 consecutive days) than control mice ($t(6) = 2.64$, $P = 0.0386$; Fig. 3a). sH-2D-expressing mice also performed more trials ($t(6) = 3.35$, $P = 0.0154$; Fig. 3b), normal trials ($t(6) = 2.64$, $P = 0.0386$; Fig. 3c), and correction trials ($t(6) = 3.58$, $P = 0.0116$; Fig. 3d). Mice were then subjected to reversal learning. In a 9-day reversal learning task, no significant differences were observed in the percentage of correct responses (group, $F(1, 3) = 0.24$, $P = 0.6565$; sessions, $F(8, 24) = 38.88$, $P < 0.01$; group × sessions, $F(8, 24) = 1.80$, $P = 0.1272$; Fig. 3e) or the perseveration index (group, $F(1, 3) = 0.7183$, $P = 0.71$; sessions, $F(8, 24) = 9.14$, $P < 0.0001$; group × sessions, $F(8, 24) = 0.40$, $P = 0.9096$; Fig. 3f) between the two groups of mice.

Morphology of DMS and DLS neurons in sH-2D-expressing mice

The dorsal striatum is anatomically divided into DMS and DLS. These areas are involved in VD learning [20, 23]. These striatal regions receive excitatory inputs from two major sources, the cortex and thalamus,

which control contextual, motor, and perceptual decisions [26, 34]. Therefore, we analyzed the morphology of DMS and DLS neurons in control and sH-2D-expressing mice by the Sholl analysis (Fig. 4a and 4f). The dendrites of DMS neurons in sH-2D-expressing mice showed significantly fewer intersections (group, $F(1, 22) = 27.79$, $P < 0.0001$; intersection, $F(5, 110) = 14.04$, $P < 0.0001$; group × intersection interaction, $F(5, 110) = 1.173$, $P = 0.3271$; Fig. 4b), shorter lengths (group, $F(1, 22) = 28.70$, $P < 0.0001$; length, $F(5, 110) = 17.53$, $P < 0.0001$; group × length, $F(5, 110) = 1.870$, $P = 0.1053$; Fig. 4c), and less nodes (group, $F(1, 22) = 28.39$, $P < 0.0001$; node, $F(5, 110) = 7.018$, < 0.0001; group × node, $F(5, 110) = 1.746$, $P = 0.1301$; Fig. 4d) and endings (group, $F(1, 22) = 26.82$, $P < 0.0001$; ending, $F(5, 110) = 10.60$, $P < 0.0001$; group × ending, $F(5, 110) = 1.23$; $P = 0.3000$; Fig. 4e) per Sholl segment, particularly those 10–60 μm from the soma, than those in control mice. Similarly, the dendrites of DLS neurons in sH-2D-expressing mice showed significantly fewer intersections (group, $F(1, 22) = 26.71$, $P < 0.0001$; intersection, $F(5, 110) = 17.57$, < 0.0001; group × intersection, $F(5, 110) = 1.543$, $P = 0.1824$; Fig. 4g), shorter lengths (group, $F(1, 22) = 32.42$, < 0.0001; length, $F(5, 110) = 22.38$, < 0.0001; group × length, $F(5, 110) = 2.457$, $P = 0.0376$; Fig. 4h), and less nodes (group, $F(1, 22) = 9.79$, < 0.0001; node, $F(5, 110) = 12.63$, $P < 0.01$; group × node, $F(5, 110) = 1.54$, $P = 0.1844$; Fig. 4i) and endings (group, $F(1, 22) = 15.99$, $P = 0.0006$; ending, $F(5, 110) = 10.48$, < 0.0001; group × ending, $F(5, 110) = 2.14$, $P = 0.0664$; Fig. 4j) per Sholl segment than those in control mice.

Effects of clozapine on behavioral deficits in sH-2D-expressing mice

We previously reported that sH-2D-expressing mice showed impaired social behavior and objection recognition memory in social interaction and novel object recognition tests, respectively (Sobue et al., 2018). To elucidate the relationships between these behavioral changes in sH-2D-expressing mice and the clinical symptoms of mental diseases, the effects of clozapine (5.0 mg/kg; oral administration), an atypical antipsychotic drug, were analyzed. sH-2D-expressing mice were treated with clozapine 60 min before the tasks [35]. In the social interaction test, clozapine significantly attenuated dysfunctions in social activity in sH-2D-expressing mice, while the same treatment had negligible effects on social behavior in control mice (group, $F(1, 33) = 17.4$, $p < 0.0001$; trials, $F(3, 99) = 88.3$, $p < 0.0001$; treatment, $F(1, 33) = 1.15$, $p = 0.2911$; trials × AAV-type, $F(3, 99) = 10.7$, $p < 0.0001$; trials × Treatment, $F(3, 99) = 0.44$, $p = 0.6100$; group × treatment, $F(1, 33) = 12.6$, $p < 0.0001$); trials × group × treatment, $F(3, 99) = 6.11$, $p < 0.0001$; Fig. 5a). Impaired object recognition memory in sH-2D-expressing mice was also significantly ameliorated by the treatment with clozapine (group, $F(1,33) = 22.4$, $P < 0.0001$; treatment, $F(1,33) = 10.4$, $P < 0.0001$, group × treatment, $F(1,33) = 14.14$, $p < 0.0001$; Fig. 5b).

Discussion

Touchscreen-based behavioral assays are parallel with computerized tasks used in human patients [18, 36]. Mice carrying human disease-related genetic mutations exhibit cognitive impairments in the touchscreen-based VD task [19–22, 37]. Previous studies suggested that normal performance in the VD task depends on the intact function of the corticostriatal circuit [20, 23], which consists of the PFC,

striatum, and thalamus, and is considered to be important for learning behaviors in humans, primates, and rodents [38–40]. Therefore, the function of the mPFC was tested using the VD task, which relies on this area and its projection terminals, to assess the impact of the astrocyte pathology and resulting behavioral changes on the computation of cognitive outputs with a high translational validity. The first novel result of the present study is regional and cell specificities in the role of astroglial MHCI in the touchscreen-based VD task. The animal model used here allowed astrocytes to be specifically targeted within the mPFC, without affecting other types of cells, by using the AAV under the control of the GFAP promotor [17].

The task started with 5 stages of pretraining prior to the VD task. By gradually completing the 5 stages, mice learned how to operate the touchscreen to get a reward. The results obtained showed that the performance of sH-2D-expressing mice was normal in the response phase sessions (stages 1–4), but impaired in the punish phase session (stage 5). Therefore, sH-2D-expressing mice appear to have normal visuospatial and motor functions, but impaired reward-associated discriminative learning. Similar to stage 5, the VD task requires learning one of two stimuli (marble and fan) simultaneously displayed on the screen is associated with the reward. The total numbers of sessions, trials, normal trials, and correction trails were significantly higher in sH-2D-expressing mice than in control mice, indicating that reward learning was significantly impaired by the overexpression of MHCI in astrocytes in the mPFC. However, no significant differences were observed between sH-2D-expressing mice and control mice in the performance of reversal learning, in which the previously incorrect stimulus becomes the correct stimulus and vice versa. The perseveration index, a paradigm that is often used in reversal learning to evaluate behavioral flexibility in mice, was also similar between two groups of mice. Astrocyte pathology in the mPFC affects attention and reversal learning functions [41, 42], and lesions in the mPFC have a negative impact on the performance of reversal learning [43]. These findings suggest a critical role for the mPFC in reversal learning. Accordingly, the normal capability for reversal learning in sH-2D-expressing mice indicates that behavioral flexibility was minimally affected by the overexpression of astroglial MHCI in the mPFC.

Astrocytes play critical roles in CNS homeostasis by supporting neuronal metabolism and excitability, structuring the blood-brain-barrier, and limiting the synapse microenvironment [44]. They provide neurotrophic support, promote synapse formation and plasticity, and regulate synaptic transmission by interacting with dendritic spines and neuronal cell bodies [45–47]. We previously reported that spine density in the mPFC was significantly lower in sH-2D-expressing mice than in control mice, which may have had a negative impact on VD learning in sH-2D-expressing mice [17].

Corticostriatal projections are massive and broad and arise from all cortical regions [48, 49]. Pyramidal neurons in the mPFC provide cortical input, and their axons terminate primarily on the spines of medium spiny neurons, more than 90% of which consist of a striatal neuronal population [48]. Instrumental action and outcome behaviors depend on the striatum and its connections with the mPFC [24, 25]. Neuronal manipulations or lesion studies demonstrated that the dorsal striatum is associated with VD learning [20, 23]. Cortical synaptic inputs into the striatum are important for the maturation of the dendritic

arborization of striatal spine projection neurons [50]. In glutamatergic neurotransmission, astrocytes contribute to the synthesis of glutamine [51], and are a known store of glycogen, an energy precursor that supports neuronal activity in the brain [52]. Striatal medium spiny neurons receive glutamatergic excitatory inputs from vesicular glutamate transport 1-positive corticostriatal neurons [53], while astrocytes in all of these brain regions are capable of the vesicular release of glutamate [54]. The present results showed that the overexpression of MHCI in astrocytes in the mPFC significantly decreased the dendritic complexity of striatal medium spiny neurons, suggesting that the astrocyte pathology in the mPFC affects corticostriatal projections. Accordingly, the overexpression of astroglial MHCI in the mPFC may alter corticostriatal glutamatergic neurons, followed by reductions in dendritic complexity in the striatum and ultimately impair VD learning. More direct evidence is needed to confirm this in future studies.

We previously demonstrated that a treatment with polyinosinic-polycytidylic acid (poly:C) in adult mice significantly increased MCHI, interferon, tumor necrosis factor-a, and interleukin-6 mRNA expression levels in the mPFC [17]. Activated microglia induce neuronal degeneration or death, both of which are associated with mental disorders such as schizophrenia and depression [55–57]. Under pathological conditions, astrocytes secrete several inflammatory cytokines and chemokines that interrupt local immune responses, which may contribute to the expansion of primary lesions, leading to further neuronal loss [58, 59].

Clozapine, an atypical antipsychotic drug, exerts antagonistic effects on multiple neurotransmitter receptors, such as serotonin 5-HT2, muscarinic M1, and dopamine D1, D2, and D4 receptors, and attenuates behavioral impairments in animal models of schizophrenia, including the neonatal polyI:C treatment model [60]. This antipsychotic drug has been reported to exhibit anti-inflammatory activities, and decrease astrocyte and microglial activation [61, 62]. Thus, clozapine protects neurons from the inflammatory changes induced by poly I:C and prevents increases in interleukin-6 levels in the rodent brain [63, 64]. Behavioral abnormalities in sH-2D-expressing mice as well as their sensitivity to clozapine suggest their face and predictive validities as an animal model of schizophrenia. In terms of construct validity, association studies have implicated MHCI genes in several neuropsychiatric disorders including schizophrenia [3, 11, 65]. Furthermore, the ameliorating effects of clozapine on behavioral abnormalities in sH-2D-expressing mice indicate its anti-inflammatory activity and role in neurotransmitter systems, including the dopaminergic neuronal system, which is involved in the astrocyte pathology [66]. Further studies are needed to confirm the effects of clozapine on behavioral and neuronal dysfunctions in sH-2D-expressing mice.

Conclusion

In conclusion, the present results suggest that the overexpression of MHCI in astrocytes in the mPFC results in impaired VD learning, which is associated with decreased dendritic complexity in medium spine neurons in the dorsal striatum and mPFC.

Abbreviations

AAV, adeno-associated virus; CNS, central nervous system; DLS, dorsolateral striatum; DMS, dorsomedial striatum; GFAP, glial fibrillary acidic protein; ITI, inter-trial interval; MHC, major histocompatibility complex; MHCI, MHC class I; PCR, polymerase chain reaction; VD, visual discrimination; mPFC, media prefrontal cortex; poly
C, polyinosinic-polycytidylic acid; sH-2D, soluble form of H-2D; sH-2D-expressing mice, Mice expressing the soluble form of H-2D in the mPFC.

Declarations

Ethics approval and consent to participate

Animals were handled in accordance with the guidelines established by the Institutional Animal Care and Use Committee of Nagoya University, the Guiding Principles for the Care and Use of Laboratory Animals approved by the Japanese Pharmacological Society, and the National Institutes of Health Guide for the Care and Use of Laboratory Animals.

Consent for publication

Not applicable.

Availability of data and materials

All data used in this study are available from the corresponding author on reasonable request.

Competing interests

None of the authors have any conflicts of interests related to this work.

Funding

This work was supported by the following funding sources: KAKENHI Grant Numbers JP17H01380, JP17H02220, JP17H04031, 17H04031, 20H03428 and JP17H04252, from Japan Society for the Promotion of Science, 19dm0107087h0004 and 19mk0101156h0001 from Japan Agency for Medical Research and Development, and from The Uehara Memorial Foundation.

Author contributions

B.W. and K.H. devised the project and the main conceptual ideas, participated in all experiments and drafted the manuscript. A.S. and N.I. assisted with experiments. To.N. contributed to the manuscript discussion. Ta.N. and K.Y. supervised the work and finalized the manuscript.

Acknowledgments

B.W. was personally supported by an Ajinomoto Scholarship Foundation and the Otsuka Toshimi Scholarship Foundation.

References

1. Murphy JB, Sturm E. Conditions Determining the Transplantability of Tissues in the Brain. J Exp Med. 1923;38:183–97.
2. Joly E, Mucke L, Oldstone MB. Viral persistence in neurons explained by lack of major histocompatibility class I expression. Science. 1991;253:1283–5.
3. Garay PA, McAllister AK. Novel roles for immune molecules in neural development: implications for neurodevelopmental disorders. Front Synaptic Neurosci. 2010;2:136.
4. Stevens B, Allen NJ, Vazquez LE, Howell GR, Christopherson KS, Nouri N, Micheva KD, Mehalow AK, Huberman AD, Stafford B, et al. The classical complement cascade mediates CNS synapse elimination. Cell. 2007;131:1164–78.
5. Shatz CJ. MHC class I: an unexpected role in neuronal plasticity. Neuron. 2009;64:40–5.
6. Heemels MT, Ploegh H. Generation, translocation, and presentation of MHC class I-restricted peptides. Annu Rev Biochem. 1995;64:463–91.
7. Natarajan K, Li H, Mariuzza RA, Margulies DH. MHC class I molecules, structure and function. Rev Immunogenet. 1999;1:32–46.
8. Fleischer B, Wagner H. Significance of T4 or T8 phenotype of human cytotoxic T-lymphocyte clones. Curr Top Microbiol Immunol. 1986;126:101–9.
9. Pawelec G, Schneider EM, Rehbein A, Balko I, Wernet P. Dissection of suppressor cell generation in vitro. Hum Immunol. 1986;17:343–54.
10. Boulanger LM. MHC class I in activity-dependent structural and functional plasticity. Neuron Glia Biol. 2004;1:283–9.
11. Elmer BM, Estes ML, Barrow SL, McAllister AK. MHCI requires MEF2 transcription factors to negatively regulate synapse density during development and in disease. J Neurosci. 2013;33:13791–804.
12. Lee H, Brott BK, Kirkby LA, Adelson JD, Cheng S, Feller MB, Datwani A, Shatz CJ. Synapse elimination and learning rules co-regulated by MHC class I H2-Db. Nature. 2014;509:195–200.
13. Biesmans S, Meert TF, Bouwknecht JA, Acton PD, Davoodi N, De Haes P, Kuijlaars J, Langlois X, Matthews LJ, Ver Donck L, et al. Systemic immune activation leads to neuroinflammation and sickness behavior in mice. Mediators Inflamm. 2013;2013:271359.
14. Norden DM, Trojanowski PJ, Walker FR, Godbout JP. Insensitivity of astrocytes to interleukin 10 signaling following peripheral immune challenge results in prolonged microglial activation in the aged brain. Neurobiol Aging. 2016;44:22–41.
15. Foster JA, Quan N, Stern EL, Kristensson K, Herkenham M. Induced neuronal expression of class I major histocompatibility complex mRNA in acute and chronic inflammation models. J

Neuroimmunol. 2002;131:83–91.

16. Ng YK, Ling EA. Induction of major histocompatibility class II antigen on microglial cells in postnatal and adult rats following intraperitoneal injections of lipopolysaccharide. Neurosci Res. 1997;28:111–8.
17. Sobue A, Ito N, Nagai T, Shan W, Hada K, Nakajima A, Murakami Y, Mouri A, Yamamoto Y, Nabeshima T, et al. Astroglial major histocompatibility complex class I following immune activation leads to behavioral and neuropathological changes. Glia. 2018;66:1034–52.
18. Bussey TJ, Holmes A, Lyon L, Mar AC, McAllister KA, Nithianantharajah J, Oomen CA, Saksida LM. New translational assays for preclinical modelling of cognition in schizophrenia: the touchscreen testing method for mice and rats. Neuropharmacology. 2012;62:1191–203.
19. Nithianantharajah J, McKechanie AG, Stewart TJ, Johnstone M, Blackwood DH, St Clair D, Grant SG, Bussey TJ, Saksida LM. Bridging the translational divide: identical cognitive touchscreen testing in mice and humans carrying mutations in a disease-relevant homologous gene. Sci Rep. 2015;5:14613.
20. Wulaer B, Nagai T, Sobue A, Itoh N, Kuroda K, Kaibuchi K, Nabeshima T, Yamada K. Repetitive and compulsive-like behaviors lead to cognitive dysfunction in Disc1(Delta2-3/Delta2-3) mice. Genes Brain Behav. 2018;17:e12478.
21. Nithianantharajah J, Komiyama NH, McKechanie A, Johnstone M, Blackwood DH, St Clair D, Emes RD, van de Lagemaat LN, Saksida LM, Bussey TJ, Grant SG. Synaptic scaffold evolution generated components of vertebrate cognitive complexity. Nat Neurosci. 2013;16:16–24.
22. Saito R, Koebis M, Nagai T, Shimizu K, Liao J, Wulaer B, Sugaya Y, Nagahama K, Uesaka N, Kushima I, et al: **Comprehensive analysis of a novel mouse model of the 22q11.2 deletion syndrome: a model with the most common 3.0-Mb deletion at the human 22q11.2 locus**. Transl Psychiatry 2020, **10**:35.
23. Brigman JL, Daut RA, Wright T, Gunduz-Cinar O, Graybeal C, Davis MI, Jiang Z, Saksida LM, Jinde S, Pease M, et al. GluN2B in corticostriatal circuits governs choice learning and choice shifting. Nat Neurosci. 2013;16:1101–10.
24. Corbit LH, Nie H, Janak PH. Habitual alcohol seeking: time course and the contribution of subregions of the dorsal striatum. Biol Psychiatry. 2012;72:389–95.
25. Murray JE, Belin D, Everitt BJ. Double dissociation of the dorsomedial and dorsolateral striatal control over the acquisition and performance of cocaine seeking. Neuropsychopharmacology. 2012;37:2456–66.
26. Cox J, Witten IB. Striatal circuits for reward learning and decision-making. Nat Rev Neurosci. 2019;20:482–94.
27. Meziane H, Ouagazzal AM, Aubert L, Wietrzych M, Krezel W. Estrous cycle effects on behavior of C57BL/6J and BALB/cByJ female mice: implications for phenotyping strategies. Genes Brain Behav. 2007;6:192–200.
28. Nagai T, Nakamuta S, Kuroda K, Nakauchi S, Nishioka T, Takano T, Zhang X, Tsuboi D, Funahashi Y, Nakano T, et al. Phosphoproteomics of the Dopamine Pathway Enables Discovery of Rap1 Activation

as a Reward Signal In Vivo. Neuron. 2016;89:550–65.

29. Paxinos G, Franklin KBJ: The Mouse Brain in Stereotaxic Coordinates. Elsevier Academic Press; 2004.
30. Horner AE, Heath CJ, Hvoslef-Eide M, Kent BA, Kim CH, Nilsson SR, Alsio J, Oomen CA, Holmes A, Saksida LM, Bussey TJ. The touchscreen operant platform for testing learning and memory in rats and mice. Nat Protoc. 2013;8:1961–84.
31. Ibi D, Nagai T, Kitahara Y, Mizoguchi H, Koike H, Shiraki A, Takuma K, Kamei H, Noda Y, Nitta A, et al. Neonatal polyI:C treatment in mice results in schizophrenia-like behavioral and neurochemical abnormalities in adulthood. Neurosci Res. 2009;64:297–305.
32. Nagai T, Takuma K, Kamei H, Ito Y, Nakamichi N, Ibi D, Nakanishi Y, Murai M, Mizoguchi H, Nabeshima T, Yamada K. Dopamine D1 receptors regulate protein synthesis-dependent long-term recognition memory via extracellular signal-regulated kinase 1/2 in the prefrontal cortex. Learn Mem. 2007;14:117–25.
33. Huber PJ. Robust statistical procedures. 2nd ed. Philadelphia: Society for Industrial and Applied Mathematics; 1996.
34. Smith Y, Surmeier DJ, Redgrave P, Kimura M. Thalamic contributions to Basal Ganglia-related behavioral switching and reinforcement. J Neurosci. 2011;31:16102–6.
35. Kitagawa K, Nagai T, Yamada K. Pharmacological and proteomic analyses of neonatal polyI:C-treated adult mice. Neurosci Res. 2019;147:39–47.
36. Hvoslef-Eide M, Mar AC, Nilsson SR, Alsio J, Heath CJ, Saksida LM, Robbins TW, Bussey TJ. The NEWMEDS rodent touchscreen test battery for cognition relevant to schizophrenia. Psychopharmacology. 2015;232:3853–72.
37. Yang M, Lewis FC, Sarvi MS, Foley GM, Crawley JN. 16p11.2 Deletion mice display cognitive deficits in touchscreen learning and novelty recognition tasks. Learn Mem. 2015;22:622–32.
38. Haber SN. The place of dopamine in the cortico-basal ganglia circuit. Neuroscience. 2014;282:248–57.
39. Gunaydin LA, Kreitzer AC. Cortico-Basal Ganglia Circuit Function in Psychiatric Disease. Annu Rev Physiol. 2016;78:327–50.
40. Ng TH, Alloy LB, Smith DV. Meta-analysis of reward processing in major depressive disorder reveals distinct abnormalities within the reward circuit. Transl Psychiatry. 2019;9:293.
41. Birrell JM, Brown VJ. Medial frontal cortex mediates perceptual attentional set shifting in the rat. J Neurosci. 2000;20:4320–4.
42. Nagai J, Rajbhandari AK, Gangwani MR, Hachisuka A, Coppola G, Masmanidis SC, Fanselow MS, Khakh BS. Hyperactivity with Disrupted Attention by Activation of an Astrocyte Synaptogenic Cue. Cell. 2019;177:1280–92 e1220.
43. Latif-Hernandez A, Shah D, Ahmed T, Lo AC, Callaerts-Vegh Z, Van der Linden A, Balschun D, D'Hooge R. Quinolinic acid injection in mouse medial prefrontal cortex affects reversal learning abilities,

cortical connectivity and hippocampal synaptic plasticity. Sci Rep. 2016;6:36489.

44. Colombo E, Farina C. Astrocytes: Key Regulators of Neuroinflammation. Trends Immunol. 2016;37:608–20.
45. Ben Achour S, Pascual O. Astrocyte-neuron communication: functional consequences. Neurochem Res. 2012;37:2464–73.
46. Freeman MR, Rowitch DH. Evolving concepts of gliogenesis: a look way back and ahead to the next 25 years. Neuron. 2013;80:613–23.
47. Haber M, Zhou L, Murai KK. Cooperative astrocyte and dendritic spine dynamics at hippocampal excitatory synapses. J Neurosci. 2006;26:8881–91.
48. Bolam JP, Hanley JJ, Booth PA, Bevan MD. Synaptic organisation of the basal ganglia. J Anat. 2000;196(Pt 4):527–42.
49. Albin RL, Young AB, Penney JB. The functional anatomy of basal ganglia disorders. Trends Neurosci. 1989;12:366–75.
50. Buren C, Tu G, Parsons MP, Sepers MD, Raymond LA. Influence of cortical synaptic input on striatal neuronal dendritic arborization and sensitivity to excitotoxicity in corticostriatal coculture. J Neurophysiol. 2016;116:380–90.
51. Schousboe A, Sickmann HM, Bak LK, Schousboe I, Jajo FS, Faek SA, Waagepetersen HS. Neuron-glia interactions in glutamatergic neurotransmission: roles of oxidative and glycolytic adenosine triphosphate as energy source. J Neurosci Res. 2011;89:1926–34.
52. Fernandez-Fernandez S, Almeida A, Bolanos JP. Antioxidant and bioenergetic coupling between neurons and astrocytes. Biochem J. 2012;443:3–11.
53. Fremeau RT Jr, Voglmaier S, Seal RP, Edwards RH. VGLUTs define subsets of excitatory neurons and suggest novel roles for glutamate. Trends Neurosci. 2004;27:98–103.
54. Ormel L, Stensrud MJ, Bergersen LH, Gundersen V. VGLUT1 is localized in astrocytic processes in several brain regions. Glia. 2012;60:229–38.
55. Monji A, Kato TA, Mizoguchi Y, Horikawa H, Seki Y, Kasai M, Yamauchi Y, Yamada S, Kanba S. Neuroinflammation in schizophrenia especially focused on the role of microglia. Prog Neuropsychopharmacol Biol Psychiatry. 2013;42:115–21.
56. Zhu X, Levasseur PR, Michaelis KA, Burfeind KG, Marks DL. A distinct brain pathway links viral RNA exposure to sickness behavior. Sci Rep. 2016;6:29885.
57. Hong H, Kim BS, Im HI. Pathophysiological Role of Neuroinflammation in Neurodegenerative Diseases and Psychiatric Disorders. Int Neurourol J. 2016;20:2–7.
58. Xie L, Yang SH. Interaction of astrocytes and T cells in physiological and pathological conditions. Brain Res. 2015;1623:63–73.
59. Becher B, Spath S, Goverman J. Cytokine networks in neuroinflammation. Nat Rev Immunol. 2017;17:49–59.

60. Nagai T, Kitahara Y, Ibi D, Nabeshima T, Sawa A, Yamada K. Effects of antipsychotics on the behavioral deficits in human dominant-negative DISC1 transgenic mice with neonatal polyI:C treatment. Behav Brain Res. 2011;225:305–10.
61. Jeon S, Kim SH, Shin SY, Lee YH. Clozapine reduces Toll-like receptor 4/NF-kappaB-mediated inflammatory responses through inhibition of calcium/calmodulin-dependent Akt activation in microglia. Prog Neuropsychopharmacol Biol Psychiatry. 2018;81:477–87.
62. Templeton N, Kivell B, McCaughey-Chapman A, Connor B, La Flamme AC. Clozapine administration enhanced functional recovery after cuprizone demyelination. PLoS One. 2019;14:e0216113.
63. Ribeiro BM, do Carmo MR, Freire RS, Rocha NF, Borella VC, de Menezes AT, Monte AS, Gomes PX, de Sousa FC, Vale ML, et al. Evidences for a progressive microglial activation and increase in iNOS expression in rats submitted to a neurodevelopmental model of schizophrenia: reversal by clozapine. Schizophr Res. 2013;151:12–9.
64. Ribeiro BMM, Chaves Filho AJM, Costa D, de Menezes AT, da Fonseca ACC, Gama CS, Moura Neto V, de Lucena DF, Vale ML, Macedo DS. N-3 polyunsaturated fatty acids and clozapine abrogates poly I: C-induced immune alterations in primary hippocampal neurons. Prog Neuropsychopharmacol Biol Psychiatry. 2019;90:186–96.
65. McAllister AK. Major histocompatibility complex I in brain development and schizophrenia. Biol Psychiatry. 2014;75:262–8.
66. Faron-Gorecka A, Gorecki A, Kusmider M, Wasylewski Z, Dziedzicka-Wasylewska M. The role of D1-D2 receptor hetero-dimerization in the mechanism of action of clozapine. Eur Neuropsychopharmacol. 2008;18:682–91.

Figures

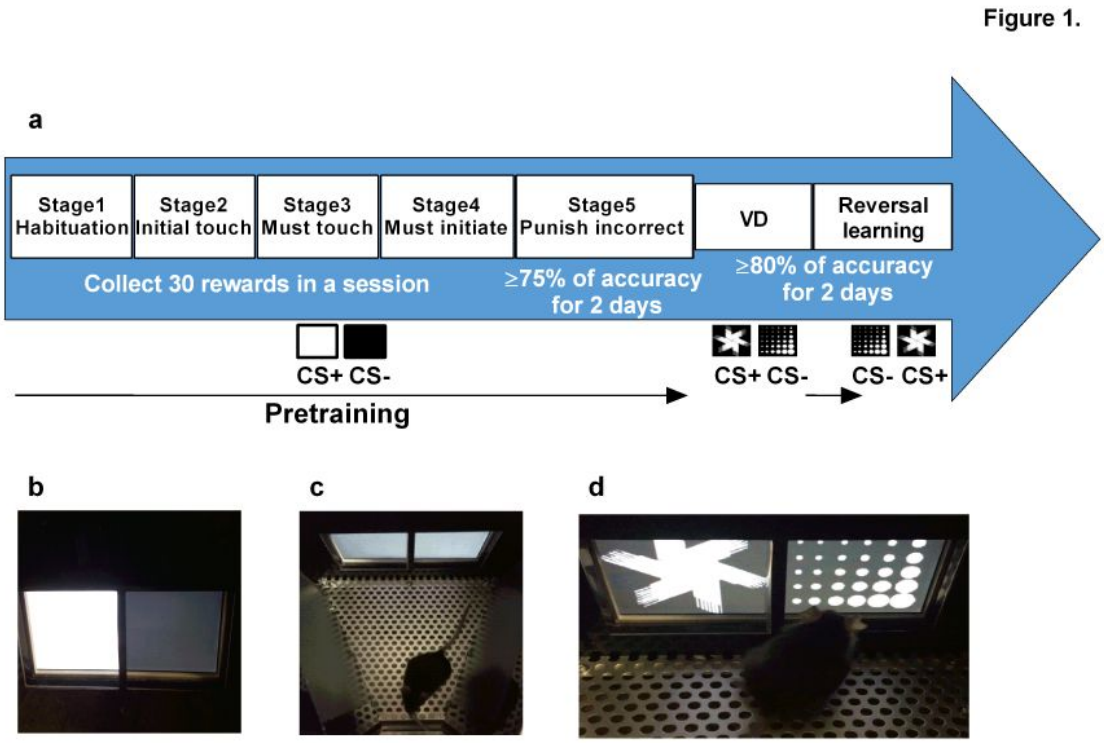

Figure 1

Experimental schedule of pretraining, VD, and reversal learning (a) Experimental schedule of pretraining, VD, and reversal learning. (b) Stimuli used in pretraining. (c) Mice initiating a new trial by touching the nozzle or receiving a liquid reward through the nozzle. (d) Mice making a decision between a pair of stimuli in VD and reversal learning. CS+, conditioned stimulus associated with a reward; CS-, unconditioned stimulus not associated with a reward; VD, visual discrimination.

Figure 2.

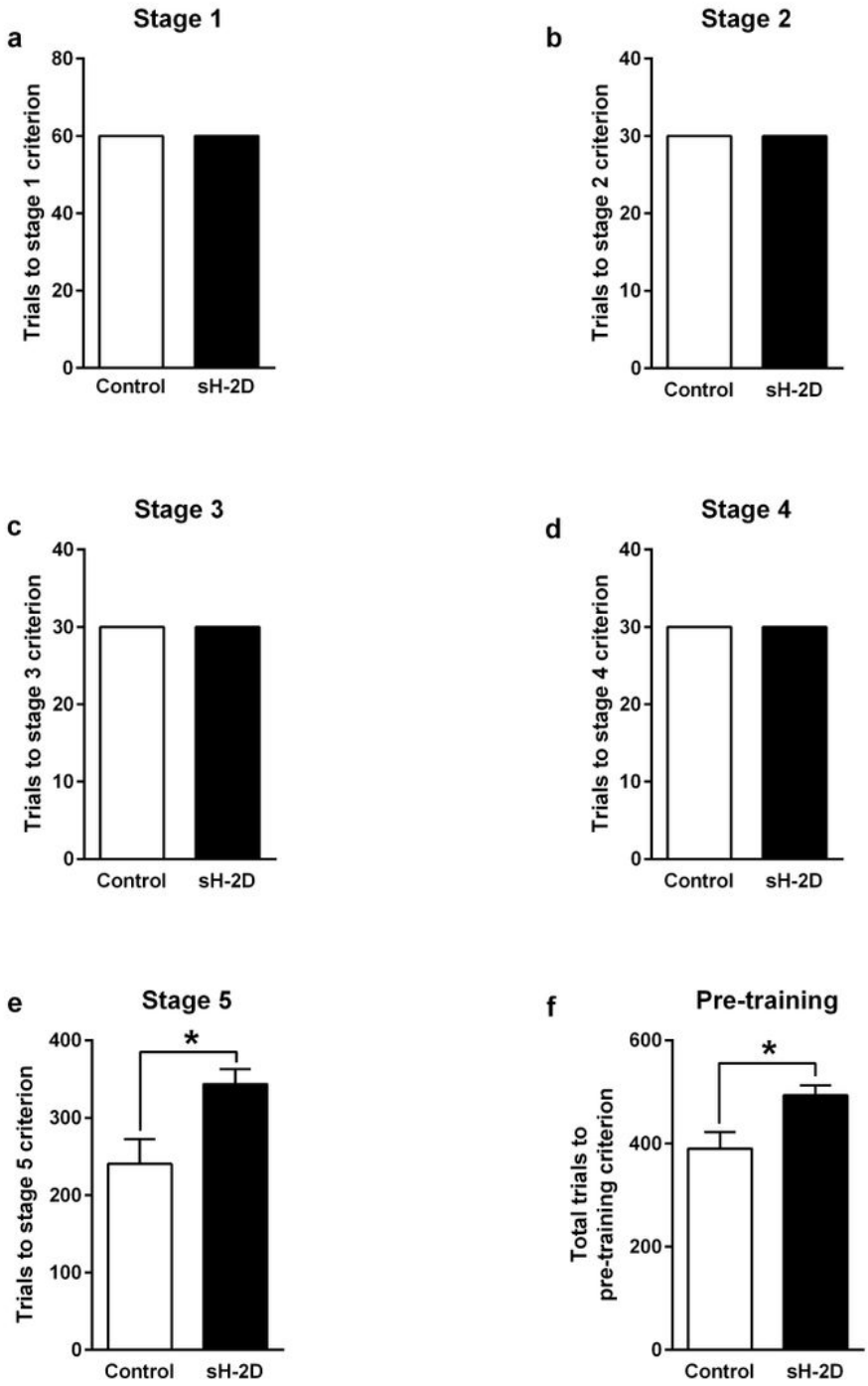

Figure 2

Performance of sH-2D-expressing mice in pretraining (a-e) Number of trials in stage 1 (a), number of trials to reach the criterion in stage 2 (b), number of trials to reach the criterion in stage 3 (c), number of trials to reach the criterion in stage 4 (d), and number of trials to reach the criterion in stage 5 (e). Total number of trials to reach the criterion in the pretraining session (f). Values indicate the mean ± SEM [Control (n = 4 mice) and sH-2D (n = 4 mice)]. *p< 0.05 significantly different from control mice.

Figure 3.

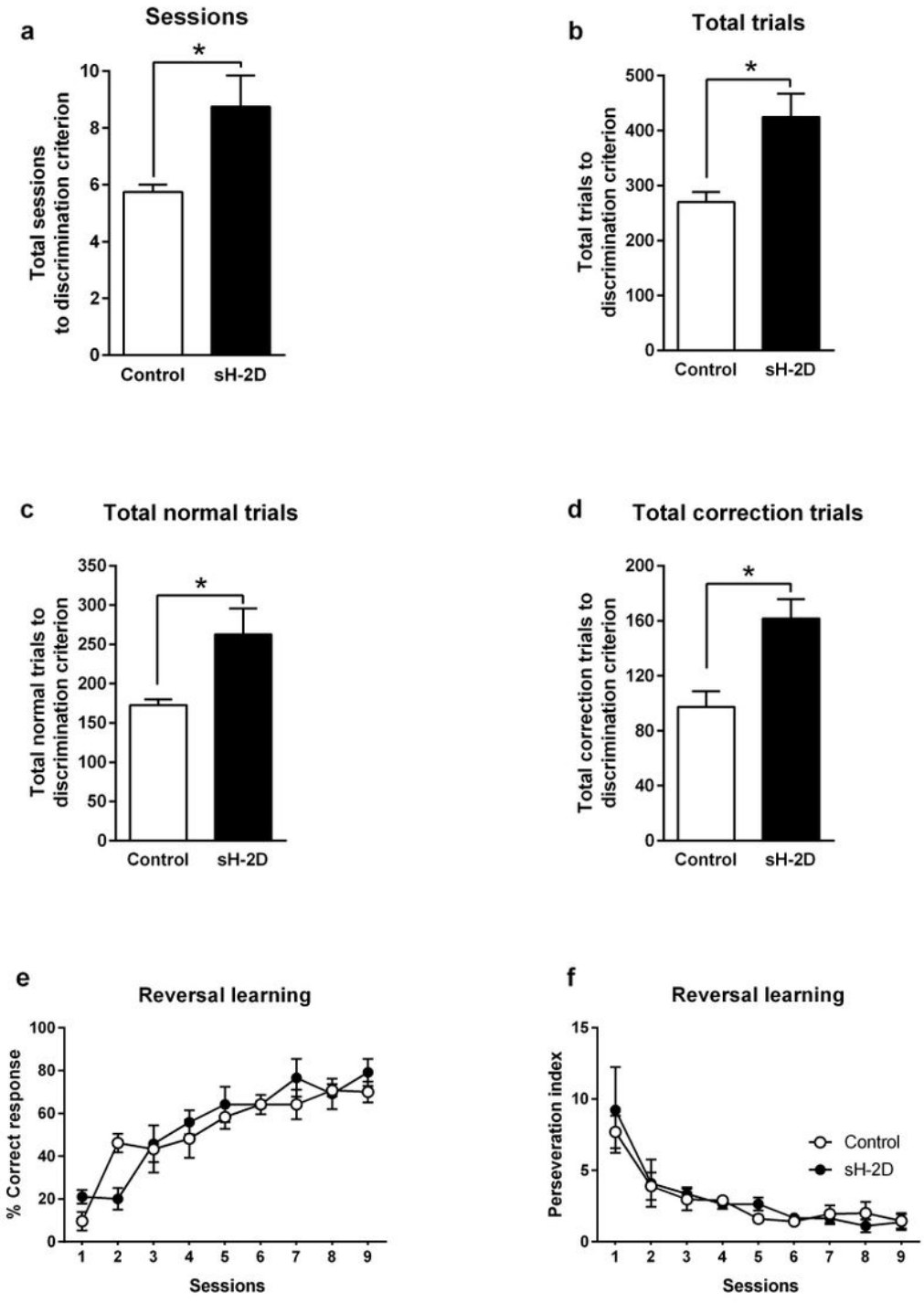

Figure 3

Performance of sH-2D-expressing mice in VD and reversal learning tasks (a-d) Performance of control and sH-2D-expressing mice in the VD task. Total number of sessions to reach the discrimination criterion (a). Total number of trials to reach the discrimination criterion (b). Total number of normal trials to reach the discrimination criterion (c). Total number of correction trials to reach the discrimination criterion (d). *p< 0.05 significantly different from control mice. (e-f) Performance of control and sH-2D-expressing mice

in reversal learning. Percentage of correct responses (e) and (f) the perseveration index during reversal learning. Values indicate the mean ± SEM [Control (n = 4 mice) and sH-2D (n = 4 mice)].

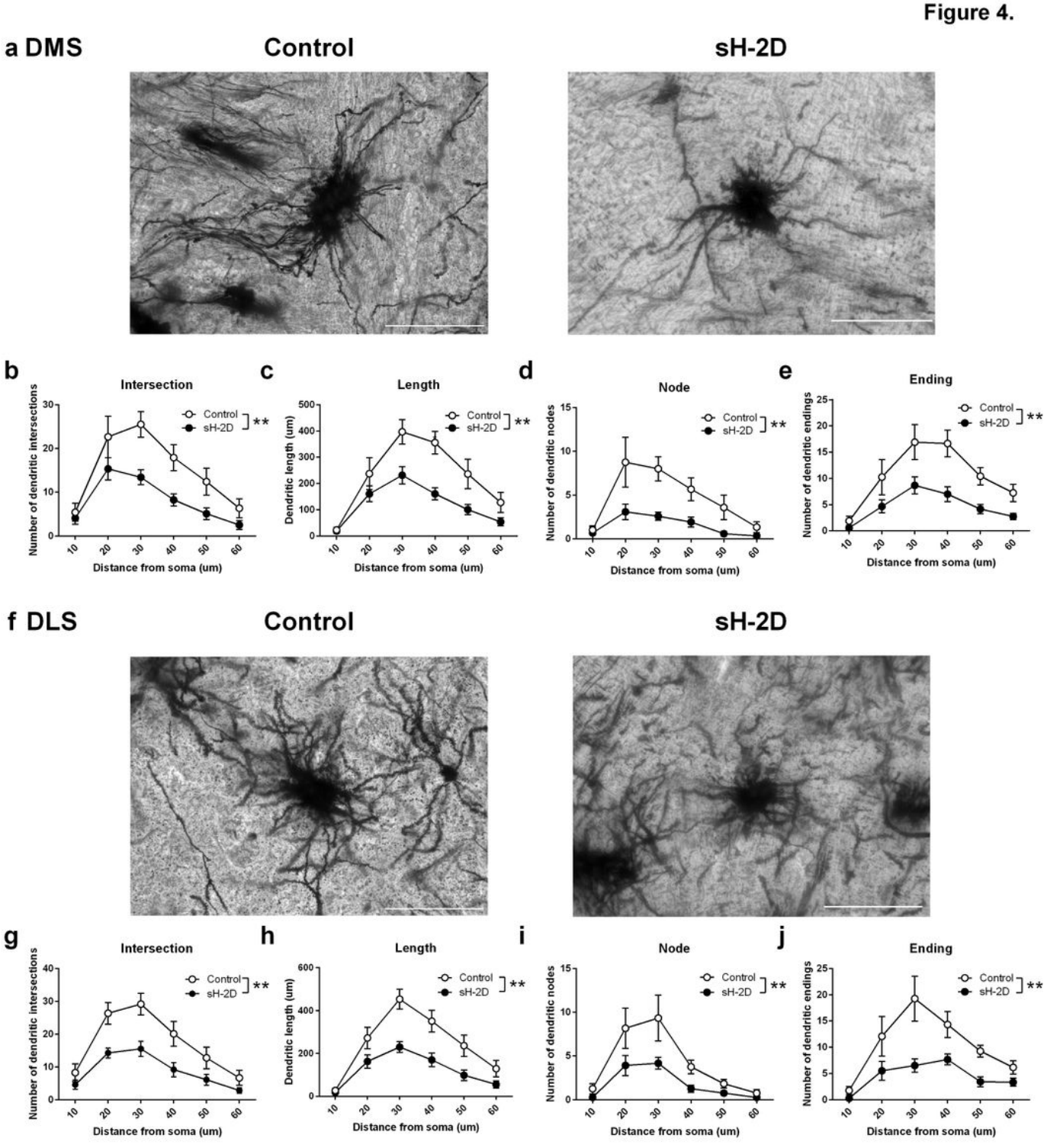

Figure 4

Morphology of DMS and DLS neurons in sH-2D-expressing mice (a) Representative images show DMS neurons in control and sH-2D-expressing mice. (b-e) Quantification of the intersection (b), length (c), node (d), and (e) ending of DMS neurons in control and sH-2D-expressing mice. (f) Representative images

showing DLS neurons in control and sH-2D-expressing mice. (g-j) Quantification of the intersection (g), length (h), node (i), and (j) ending of DMS neurons in control and sH-2D-expressing mice. **p< 0.01 significantly different from control mice. DMS, dorsomedial striatum; DLS, dorsolateral striatum. Values indicate the mean ± SEM [Control (n = 12 neurons from 4 mice) and sH-2D (n = 12 neurons from 4 mice)].

Figure 5.

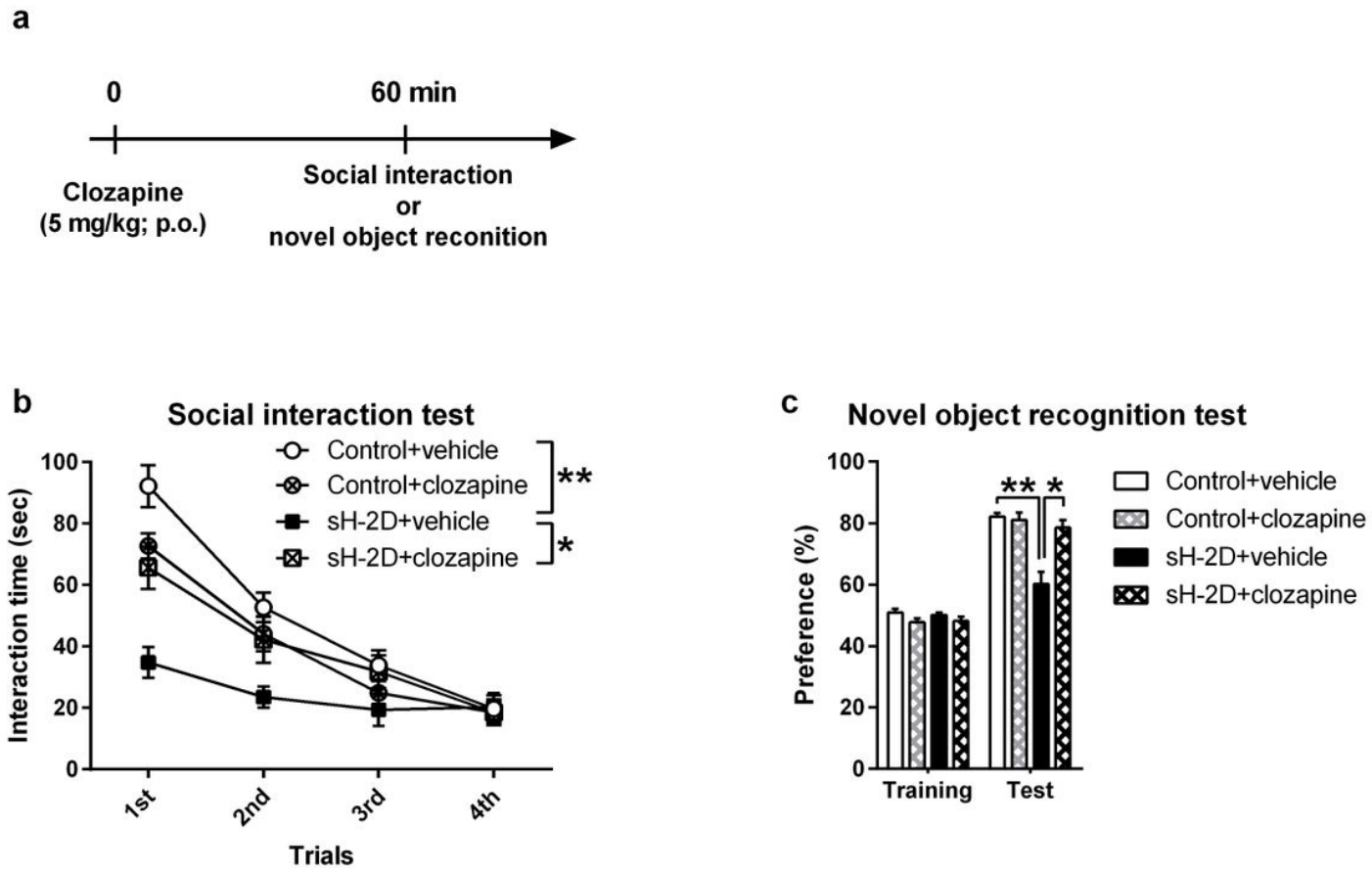

Figure 5

Effects of clozapine on behavioral deficits in sH-2D-expressing mice (a) Experimental schedule for a pharmacological study with clozapine. (b) Effects of clozapine on performance in the social interaction test in control and sH-2D-expressing mice. (c) Effects of clozapine on performance in the novel object recognition test in control and sH-2D-expressing mice. p.o., orally. *p< 0.05 or **p< 0.01 significantly different from control mice. Values indicate the mean ± SEM [control+vehicle (n = 10 mice), control+clozapine (n = 9 mice), sH-2D+vehicle (n = 9 mice), and sH-2D+clozapine (n = 9 mice)].